Macromolecular Bioscience
www.mbs-journal.de

Nanoscopic Characterization of Stearic Acid Release from Bovine Serum Albumin Hydrogels

*Niuosha Sanaeifar, Karsten Mäder, and Dariush Hinderberger**

The release behavior of 16-doxyl stearic acid (16-DSA) from hydrogels made from bovine serum albumin (BSA) is characterized. 16-DSA serves as a model tracer molecule for amphiphilic drugs. Various hydrogel preparation procedures are tested and the fatty acid release from the different gels is compared in detail. These comparisons reach from the macroscopic level, the viscoelastic behavior via rheological characterization to changes on the nanoscopic level concerning the secondary structure of the protein during gelation through infrared (ATR-IR) spectroscopy. 16-DSA-BSA interaction via continuous wave electron paramagnetic resonance (CW EPR) spectroscopy in addition gives a nanoscopic view of small molecule–hydrogel interaction. The combined effects of fatty acid concentration, hydrogel incubation time, and gelation procedures on release behavior are studied via CW EPR spectroscopy and dynamic light scattering (DLS) measurements, which provide deep insight on the interaction of 16-DSA with BSA hydrogels and the nature and size of the released components, respectively. It is found that the release rate of the fatty acid from BSA hydrogels depends on and can thus be tuned through its loading percentage, duration of hydrogel formation and the type of gelation methods. All of the results confirm the potential of these gels as delivery hosts in pharmaceutical applications allowing the sustained release of drug.

1. Introduction

Serum albumin, a small globular and in the crystalline state heart-shaped molecule is the most abundant protein in the blood stream of vertebrates.[1] From a biopharmacological point of view, albumin is a remarkably versatile (yet often low-affinity) carrier for drugs, fatty acids, and polypeptides that can attach through physical or covalent bonding to specific binding sites of this flexible protein.[2–4] Due to its low toxicity and immunogenicity, high biocompatibility, biodegradability, and considerable ligand-binding characteristics, albumin is being evaluated in many drug delivery applications.[5–7]

A wide variety of potentially therapeutically active compounds have been discovered, while only a small number of them have sufficient therapeutic effects.[8] Administration methods have a significant effect on the drug's efficacy. For instance, low bioavailability and concentration of a drug in blood plasma arises from systematic administration, which requires higher dosages or procedure repetition.[8] To overcome these barriers, controlled or directed drug delivery systems have been developed over the past few decades.[8–10] These systems should be able to release the drug at a controlled rate and sustain drug levels at the specific site for a desirable period of time.

Hydrogels are cross-linked structures made from small or polymeric molecules of biological or synthetic origin composed of numerous hydrophilic groups with the capability to absorb and preserve large amounts of water or physiological fluids within their scaffold. Due to their unique features such as high porosity and biocompatibility, hydrogels are promising candidates for a variety of biomedical applications like tissue engineering or as drug delivery systems.[8,11,12]

Albumin hydrogels have in recent years gained increased attention.[3,13,14] It is vital to choose the optimum method for preparing robust and biocompatible albumin hydrogels while maintaining the various functions of this protein such as ability to bind and release a wide range of molecules.[14] Hydrogels from serum albumin can be synthesized via thermal or pH induced methods.[15,16] The former involves conformational changes and unfolding of polypeptide segments caused by heating above denaturation temperature of the protein, which leads to hydrophobic interactions and final gel formation.[16,17] In the latter mechanism, the hydrogel is formed by lowering pH to 3.5, resulting in the aggregation of partially denatured albumin at 37 °C.[15,18,19] We have previously elucidated that hydrogel formation from bovine and for the first time human serum albumin can be achieved considerably below the protein's denaturation temperature as well as in a broader pH range than known before.[14] There are several reports on using serum albumin for drug delivery purposes, but they mostly focused on the preparation of protein nanoparticles. For

N. Sanaeifar, Prof. D. Hinderberger
Institute of Chemistry
Martin Luther University Halle-Wittenberg
Von-Danckelmann-Platz 4, Halle (Saale) 06120, Germany
E-mail: dariush.hinderberger@chemie.uni-halle.de
Prof. K. Mäder
Institute of Pharmacy
Martin Luther University Halle-Wittenberg
Wolfgang-Langenbeck-Str.4, Halle (Saale) 06120, Germany
The ORCID identification number(s) for the author(s) of this article can be found under https://doi.org/10.1002/mabi.202000126.

DOI: 10.1002/mabi.202000126

instance, Yu et al. prepared BSA nanoparticles by a desolvation method to explore the release behavior of the model dye rhodamine B.[20] Zhao et al. prepared BSA nanoparticles loaded with the cancer drug paclitaxel.[6] One study carried out by Sun and Huang described the preparation of crosslinked BSA hydrogels with intermolecular disulfide bonds. This gel could be injected through a needle and doxorubicin was used to investigate its potential in drug release applications.[18] Electron paramagnetic resonance (EPR) spectroscopy as a highly sensitive and in particular selective technique can be used to detect paramagnetic centers or free radicals.[21–23] While most of drug delivery systems cannot be studied by EPR spectroscopy directly due to lack of paramagnetic molecules, drug–protein interaction can be studied by EPR spectroscopy via use of persistent reporter radicals, so called spin labels if attached covalently or spin probes if non-covalently, into the drug, the protein or both.[21,22] One of the applications of EPR is to study the interaction of spin labeled amphiphilic molecules such as fatty acids (FAs) with proteins like serum albumin. By this method, motional parameters as well as dynamic information like binding capacity of the protein can be obtained.[24]

As explained in detail below, the mechanical properties of the albumin hydrogels show a nontrivial, rather complex dependence on the incubation time, i.e., the time at which gelation is processing a specific temperature or pH. For instance, prolonged incubation time can result in the hardening of some gels while decomposing others. The time required for gelation can be highly different, ranging from few minutes to several hours and depends on the synthetic method. In the following, the direct effect of changing the incubation time on the release rate is shown. Given that one long-term goal of this research is to develop a controlled release system based on BSA hydrogels, we have chosen 16-DSA as an amphiphilic model "drug" to investigate the release profile from the prepared gels. Mechanical properties as well as changes in the secondary structure of the synthesized gels are characterized using rheology and IR spectroscopy. In addition, we investigate the combined effects of method of gel formation, incubation time and FA concentration on the release rate. By combining the results from CW EPR spectroscopy on the interaction of fatty acids with BSA hydrogels and DLS on the released nanoscopic structures, deeper insights are obtained on the nature and size of the released components and conclusions about the release mechanisms are drawn.

2. Experimental Section

2.1. Materials

Fatty acid-free bovine serum albumin (BSA > 96%, lyophilized powder) and 16-DSA (16-doxyl stearic acid, free radical, 253596) were obtained from Sigma-Aldrich and used directly without any purification. Previously,[14] a concise and complete notation was introduced for denoting and describing physical properties of various gels as follows: $BSA_i(\Theta,p,t)$, where i specifies the gel preparation method (T = thermally induced or P = pH induced) and the three variables of temperature (Θ, in °C), pH (p) and incubation time (*t*, in minutes) are noted in parentheses. In this study the fourth parameter of time-release (in hour) referring to the release of spin probe over a period of time was added as well. For instance, $BSA_T(59, 7, 30, 24)$ indicates the gel prepared by thermal incubation at 59 °C, at pH 7 with the incubation time of 30 min studying the release 24 h after preparation.

2.2. Methods

2.2.1. Sample Preparation

BSA hydrogels were prepared by two different procedures, namely heat-induced and electrostatically/pH-induced as described previously.[14] In principle, a BSA 3×10^{-3} M (20 wt%) precursor solution was prepared by dissolving BSA powder in deionized water under stirring at 100 rpm for 1 h at room temperature. A filtration through 0.2 µm nylon filters was done to obtain a sterile solution with a pH value of 7. The 16-DSA stock solution (26×10^{-3} M) was prepared in KOH (0.1 M) and loaded to the precursor solution of BSA with different FA:BSA molar ratios (0.5:1, 1:1, and 2:1) into vials. The vials were kept in thermomixer at 65 °C and 59 °C (above and below denaturation temperature of BSA, respectively) to form heat-induced gels. For preparing pH-induced gels, HCl (2 M) was added dropwise to the solution of 16-DSA and BSA and the pH was lowered to 3.5. By this method it was possible to obtain hydrogels at 37 °C.

2.2.2. In Vitro Drug Release

For release experiments, 10 × PBS (1 mL, pH 7.4) was added on top of the synthesized hydrogels and the vials were incubated in thermomixer at 37 °C. At various time intervals, 12 µL of the release medium was taken out for further investigations and replaced by fresh PBS to maintain sink condition.

2.2.3. Rheological Characterization

The gelation kinetics and mechanical properties of synthesized hydrogels were evaluated by time-dependent rheological measurements. The starting point of gel formation is determined as the time when the storage modulus (G') increases above the loss modulus (G''), which means that the elastic properties of the gel is more noticeable than its viscous behavior. Furthermore, by investigating storage and loss moduli during gelation, it is possible to gain a deep understanding of hydrogels stability (the time after which the gel reaches the steady state), robustness and more importantly the effects of fatty acid on BSA gelation.

A Physica MCR 301 rheometer (Anton Paar, Graz, Austria) was used for these experiments. All measurements were conducted with a CP50-2/TG plate measurement system. 2000 µL of liquid samples were placed onto the rheometer plate. Silicon oil was applied to cover the measuring gap to prevent water from evaporation and the closing gap was lowered during the test. The storage and loss moduli were recorded at 0.5% oscillatory strain and 1 rad s^{-1} frequency.

2.2.4. ATR IR Spectroscopy

Attenuated total reflection (ATR) Fourier transform infrared spectroscopy (FTIR) techniques are widely used to obtain information about protein secondary structures.[25] The two major bands of proteins are amide I and amide II bands, where the former is the most sensitive band which arises mainly from the stretching vibrations of C=O bonds, and the latter originates from the bending vibration of N−H bonds.[26]

FTIR was performed to investigate changes in the secondary structure of BSA during gelation, alone and in the presence of fatty acids, respectively. 30 µL aliquot of sample were placed onto the Si-crystal plate whose temperature was controlled by a circulation water bath (HAAKE C25P thermostat). Data acquisition was commenced when the desired temperature was equilibrated. The spectra were acquired within the range of 4000–900 cm^{-1}, with 256 scans to obtain a good signal-to-noise ratio, at 4 cm^{-1} resolution by means of Bruker Tensor 27 FT-IR spectrometer equipped with a BioATRCell II and an LN-MCT photovoltaic detector and the OPUS Data Collection Program (all from Bruker, Ettlingen, Germany). To eliminate the presence of dirt, ATR cell and spectrometer were recorded in a dry atmosphere. The empty ATR cell was used as a reference. H_2O spectrum was subtracted from each spectrum at the same temperature and pH to remove the water contribution.

2.2.5. Continuous Wave Electron Paramagnetic Resonance (CW EPR) Spectroscopy

CW EPR spectroscopy was used to derive information on the released components, the release mechanisms through analysis of the interaction of fatty acids with the BSA hydrogel in bulk and in the released solution.

EPR spectroscopy is a well-suited technique to reveal the structure and dynamics of proteins, molecular self-assembly, and rotational mobility of paramagnetic molecules.[14,27,28] In this research, spin-labeled FAs were mixed into the BSA hydrogel as spin probes to characterize FA-albumin interaction and the state of the released fragments. This information can be retrieved by analyzing the rotational dynamics of the spin probe. For instance, restricted rotational motion arises from immobilized (bound) radicals, while freely tumbling spin probes indicate no or little interaction with the protein scaffold.[22] 16-DSA used as spin labels has a nitroxyl (doxyl) ring on carbon 16 of its hydrophobic chain. Previously, others and us have shown the capability of this fatty acid to be bound by both human and bovine serum albumin by various methods of loading.[14,24] Additionally, it should be mentioned that from the EPR spectroscopic point of view stearic acid (SA) and 16-DSA have very similar binding affinities to BSA.[24,29]

CW EPR measurements were recorded using a Miniscope MS400 (Magnettech, Berlin, Germany) benchtop spectrometer with a microwave power of 10 mW, a sweep width of 15 mT, and modulation amplitude of 0.2 mT. A microwave frequency of 9.4 GHz was measured using a frequency counter (Racal Dana 2101, Neu-Isenburg, Germany). All release tests were characterized at 37 °C using a temperature controller H03 (Magnettech). EPR spectra were simulated in MATLAB with the EasySpin program package to solve the Schrödinger equation for slow rotation nitroxide EPR spectra, as pioneered in the Schneider-Freed model.[30] Experimental spectra could be simulated by a weighted combination of three types of simulated EPR spectra that represent highly immobilized, intermediately bound and free FAs.

The samples were prepared by filling 12 µL solution of 16-DSA and BSA into 50 µL capillaries (Blaubrand, Wertheim, Germany), which were capped using tube sealant (Leica Critoseal).

2.2.6. Dynamic Light Scattering

Dynamic light scattering (DLS) provides information on diffusion coefficients of molecules assuming Brownian motion. DLS counts as nondestructive way to measure the hydrodynamic radius of particles using diffusive motion, size distribution, and particle sizing.[31–33] The technique of light scattering is widely established for characterization of protein, polymer structures as well as nanomaterials.[34–36]

A Litesizer 500 (Anton Paar GmbH, Graz, Austria) was used to obtain all DLS data. This device is equipped with a 40 nm semiconductor laser that irradiates samples with light of a wavelength of 658 nm. The intensity of all scattered light was measured at a 90°. Quarz cuvettes (Hellma Analytics) were used as sample holders. All measurements were conducted with 6 runs and the duration of 30 s for each run at a temperature of 37 °C with an equilibration time of 4 min.

2.2.7. Sample Preparation

To obtain the hydrodynamic radius and intensity correlation function, BSA (3×10^{-3} M) solution was prepared as described previously and diluted to different concentration by 10 × PBS. A second filtration step was included using nylon filters with a pore size of 0.2 µm to eliminate the presence of contamination and dusts. Samples were measured from release experiments to gain insight into the nature of the released particles, molecules, and gel fragments. For all measurements, 100 µL of sample were transferred into the quartz container. Release samples were tested with no further filtration.

3. Results and Discussion

3.1. General Considerations

Gels from bovine serum albumin were prepared according to the procedure reported recently.[14] To determine the release profile of the EPR active fatty acid, 16-DSA was added to BSA precursor solutions with different concentrations. Gelation of the mixture was started by elevating the temperature or reducing the pH. For the release experiments, PBS was added to the synthesized hydrogels and at certain time intervals some of the release medium was removed for further investigation.

We show in the following that incubation time during hydrogel formation plays a key role on release rate and the

type of fragments released, i.e., increasing the incubation time leads to more robust gels and lower percentage of FA release. More importantly, due to the strong gel network and inability of water to penetrate the hydrogel structure, more freely tumbling and only intermediately strong BSA-bound FAs are released from mechanically robust gels. Furthermore, increasing the FA to BSA loading ratio results in an elevated release rate for all samples.

3.2. Rheological Analysis

The suitability of a hydrogel for a certain biological or biomedical application strongly depends on its mechanical properties. The rigidity of the gel plays a significant role once it is used as a scaffold for cell adhesion and gene expression, while flowability of some hydrogels makes them excellent candidates to act as injectable carriers for drug delivery purposes.[37]

Intermolecular interactions causing the formation of protein network determine the rheological characteristics of proteins. The gelation of proteins arises from the noncovalent intermolecular forces including hydrophobic, van der Waals, solvation, and electrostatic interactions, which also govern the viscoelastic behavior of proteins.[38] Selection of all studied gels is based on our previous exploration of the gel phases, shown in detail in ref. [14]. The time dependence of the storage (G') and loss (G'') moduli of the 20 wt% solution of BSA at various temperatures are illustrated in **Figure 1**.

Figure 1A,B shows the curves of G' and G'' for precursor solutions that were heated and then kept at 65 °C (slightly above the denaturation temperature) and 59 °C (slightly below the denaturation temperature), respectively. In both cases, the

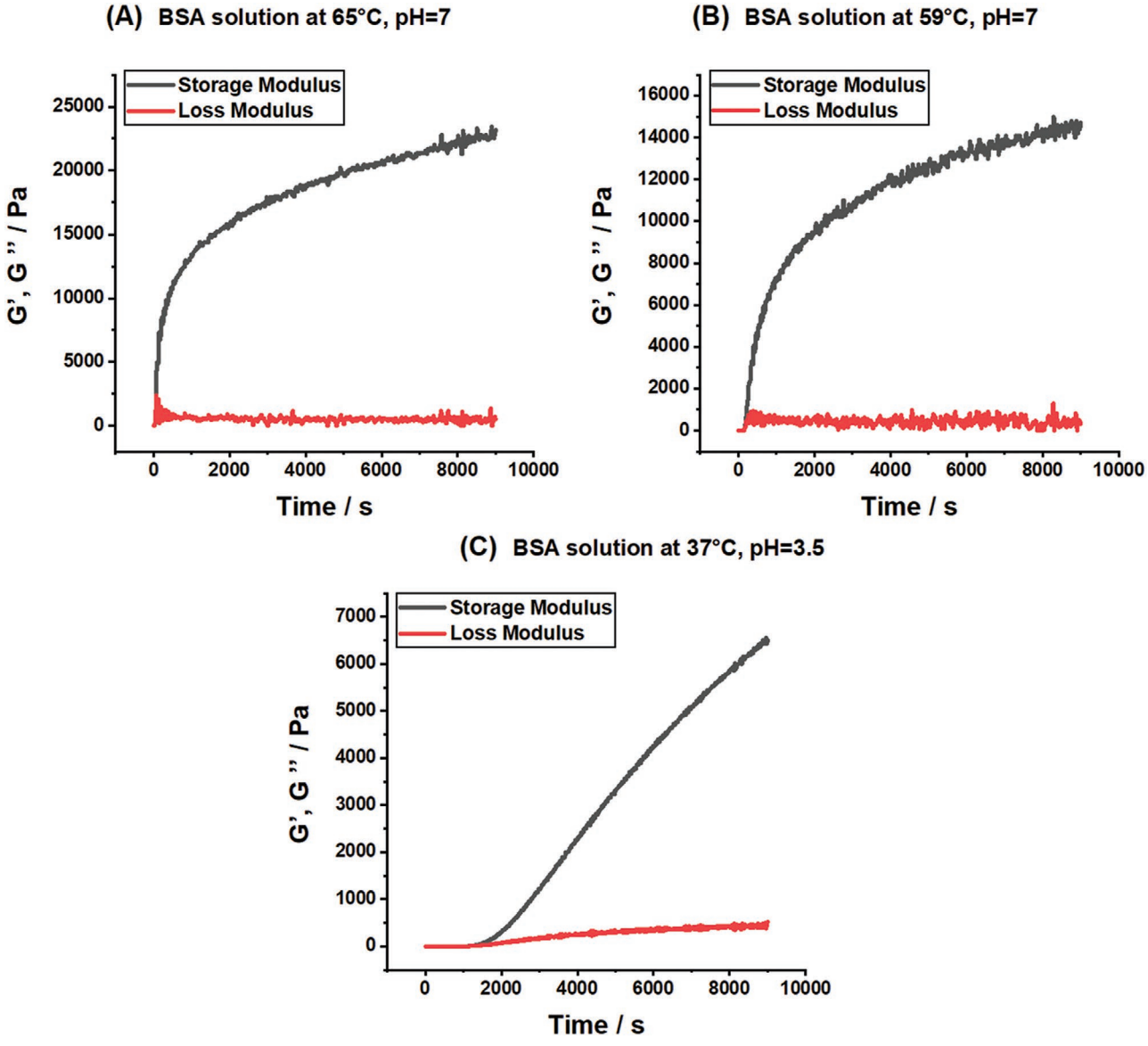

Figure 1. Time dependence of the storage (G') and loss (G'') moduli of BSA solution A) at 65 °C, pH 7, B) at 59 °C, pH 7 and C) at 37 °C, pH 3.5.

storage modulus immediately after the heating started deviates from the loss modulus which reflects the instant gel formation. We consider the gel to be mechanically tough when the value of G' exceeds 10 000 Pa after 1 h. The storage modulus for BSA_T(65,7,120) and BSA_T(59,7,120) is ≈22 000 Pa and 13 000 Pa after 2 h, respectively. Thus, it is possible to obtain robust hydrogels by the thermally induced method even at 59 °C which again shows that BSA_T-gels can form below its denaturation temperature. However, the storage modulus of the gel formed at 65 °C is considerably greater than G' value for the one prepared at 59 °C after 120 min. As can be expected, the secondary structure of serum albumin is more preserved when the hydrogel is prepared below its denaturation temperature, as is shown in the IR results below.

The mechanical properties of BSA_p(37, 3.5, t), prepared by adjusting the pH to 3.5 through the addition of HCl (2 M), are depicted in Figure 1C. No gel is formed during the first 25 min, however, at later time points, the storage modulus surpasses the loss modulus suggesting the onset of conformational changes, which results in an increase in the hydrogel robustness. This pH-induced hydrogel is less rigid than those formed by heating BSA above or close to its denaturation temperature. Furthermore, pH-triggered hydrogels require much longer incubation times to be mechanically robust and their properties are more strongly time-dependent than is the case in temperature-induced gels. Nevertheless, it is possible to obtain gels with a strong elastic network by this preparation method, although compared to the thermally induced technique, the rate of gelation is relatively slow.

The potential impact of fatty acids on albumin gel formation is investigated by adding the different ratios of stearic acid to the precursor solution of BSA_T and repeating the rheological measurements at 65 °C (see the Figure S1, Supporting Information for 59 °C and 37 °C). In accordance with previous reports,[14,39,40] it is found that fatty acids hamper thermal denaturation of the protein and stabilize the BSA molecules. Due to the presence of high affinity binding sites in albumin for interaction with fatty acids, conformational changes are impeded.

The storage and loss moduli as a function of time for the system containing BSA and stearic acid (SA) A at two different molar ratios at 65 °C are illustrated in **Figure 2**. Note that stearic acid is interchangeable with 16-DSA concerning its binding properties to BSA, as has been shown before.[14,24] The results show that the addition of stearic acids slows down gel formation and deeply affects the mechanical properties. The extent of reduction in mechanical strength depends on the concentration of SA. For example, the maximum G' value for the 0.5:1 ratio of SA:BSA is roughly half of that for BSA alone. Moreover, for the highest tested ratio of SA:BSA (2:1) the gel strength is significantly weakened. (the 1:1 SA:BSA molar ratio for various preparation methods is shown in Figure S2, Supporting Information).

3.3. BSA Conformational Changes during Hydrogel Formation

The proportions of α-helices, β-turn, and extended chain in native BSA are 67%, 10%, and 23%, respectively.[4,14,41] The composition and gelation of this protein can be affected by

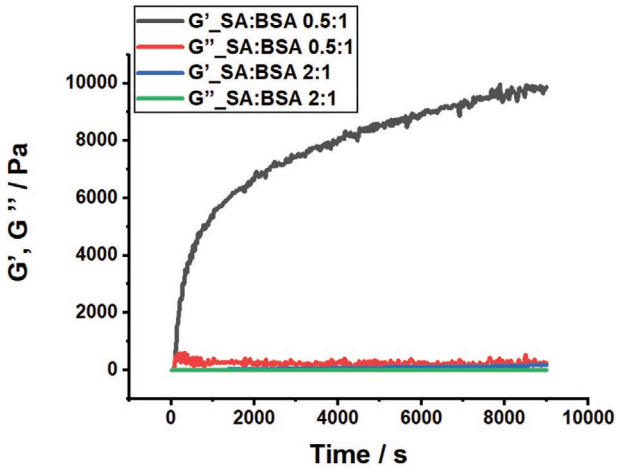

Figure 2. Time dependence of the storage (G') and loss (G'') moduli of different ratios of SA:BSA solution at 65 °C, pH 7.

environmental conditions including protein concentration, pH, temperature and addition of other solids.[14–16] For example, by heating, an increase in β-sheet content is observed while there is no β-sheet structure in native BSA. It is well known that BSA forms hydrogels at the cost of a decrease in α-helices content while that of intermolecular β-sheets increases gradually.[4,42,43] The conformational changes of BSA alone and the effect of 16-DSA on the secondary structure of this protein are studied by ATR-IR spectroscopy during the first five hours of gel formation on the plate of the ATR-IR crystal. The emergence of the two peaks at about 1620 and 1680 cm^{-1} are attributed to the vibrations of intermolecular β-sheets, the hallmark wof protein aggregation and finally gel formation.[43] As can be seen in **Figure 3**, these peaks rise for all different samples independent of gelation temperature and even the presence of 16-DSA. On the other hand, the decreasing of the band at around 1650 cm^{-1} is due to the conversion of α-helical intramolecular hydrogen bonds for intermolecular (β-sheet) hydrogen bonding formation which leads to the network structure and gelation.

To study the changes occurring in α-helix and β-sheet contents, respectively, the intensity of the peak signifying α-helical content was plotted as a function of time. By monitoring the I(α-helix)/I(β-sheet), it is possible to obtain a deeper understanding about the gelation process and structural evolution for the heat-induced method described above. Comparison of the spectrum of the hydrogel prepared at 65 °C with the one formed at 59 °C reveals that the ratio of (α-helix)/(β-sheet) is slightly lower for the former (see the plot in **Figure 4**A). This observation indicates that the structure of protein undergoes stronger changes during gelation when the temperature is above the denaturation temperature (i.e. at 65 °C). These results are comparable with the data obtained from rheology, since the G' value of the hydrogel formed at 65 °C is considerably greater than the one prepared at 59 °C, suggesting that change in secondary structure content of the individual protein and mechanical strength of the hydrogel are correlated. Furthermore, the employed ATR-IR spectrometer requires 2 min to reach the T-equilibration. This delay time is significant for gelation at 65 °C, as the gelation proceeds very quickly in these

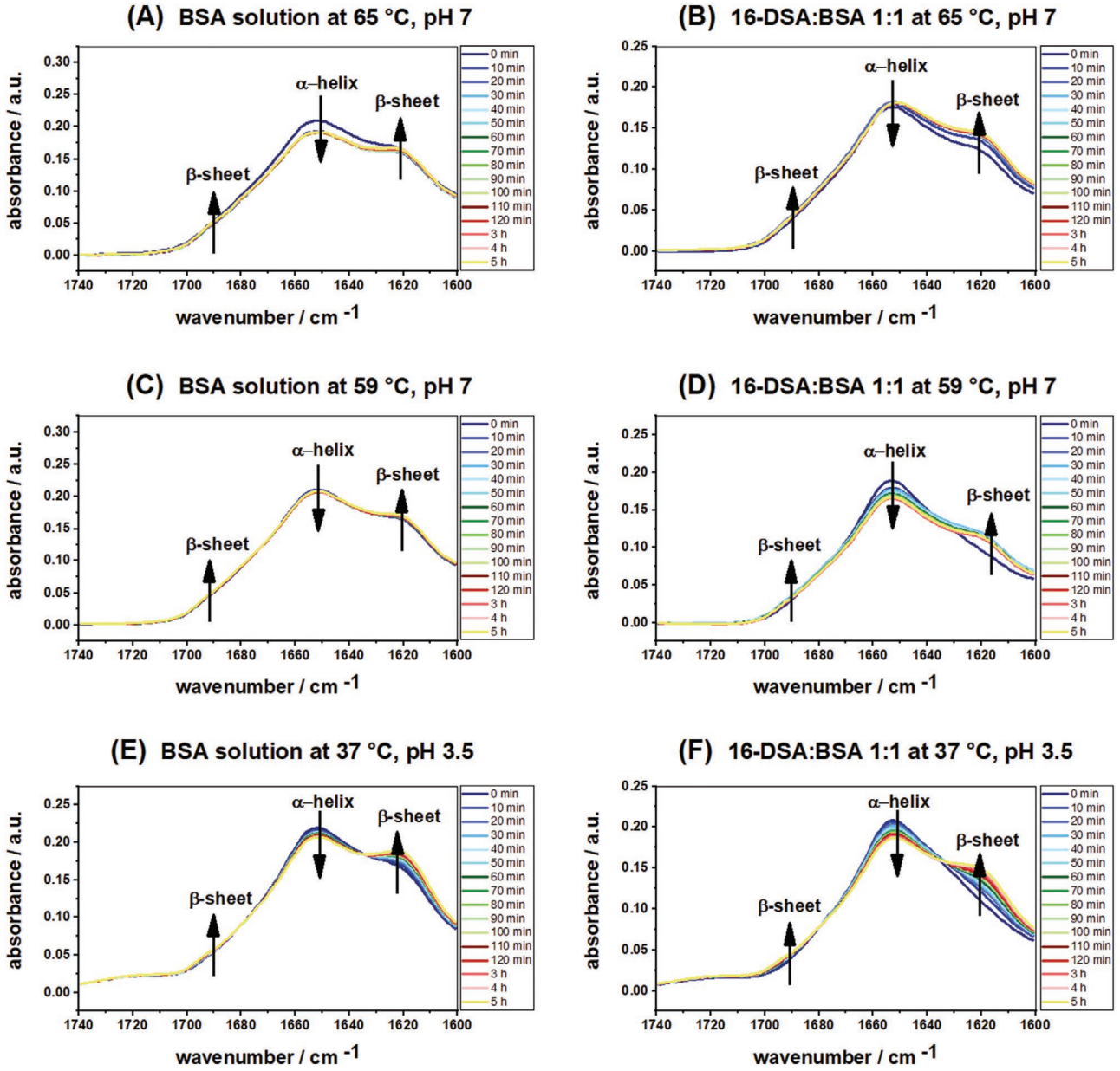

Figure 3. IR absorption spectra as a function of time for 3×10^{-3} M A) BSA precursor solution at 65 °C, pH 7, B) BSA precursor solution at a 1:1 16-DSA:BSA molar ratio at 65 °C, pH 7, C) BSA precursor solution at 59 °C, pH 7, D) BSA precursor solution at a 1:1 16-DSA:BSA molar ratio at 59 °C, pH 7, E) BSA precursor solution at 37 °C, pH 3.5 and F) BSA precursor solution at a 1:1 16-DSA:BSA molar ratio at 37 °C, pH 3.5.

first 2 min.[14] Therefore, it is hard to observe the very initial reduction in the α-helix content especially at this temperature.

Figure 4B illustrates the helix content of the $BSA_T(65,7)$, $BSA_T(59,7)$ and $BSA_P(37,3.5)$ as a function of time during gelation. We can observe that the highest α-helical content is found in the hydrogel prepared by lowering the pH to 3.5. This shows that the hydrogel formation can be affected by the pH and ionic strength of the precursor solution, as e.g. found in refs. [21] and [19]. Generally, thermally induced gels form by the transformation of α-helices into intermolecular β-sheet structures (see the Figure S3A, Supporting Information). However, in the pH triggered samples, gelation occurs by formation of β-sheet aggregates with the reduction of both, α-helix and random coil, contents (see the Figure S3B, Supporting Information). Hence, in relation, more helical content is retained in hydrogels prepared by the pH-induced technique. Furthermore, as can be seen in Figure 4B the pH-induced hydrogel does not only have a higher α-helical content but a significant downward trend during the initial hours while the heat-induced samples show a slower initial decrease in α-helix proportion and a more continuous trend later. This indicates that in all cases the majority of the conformational changes takes place during the first 50 min. However, the results from rheological measurements reveal that there is no sign of gelation for $BSA_P(37,3.5)$ in this time period. From ATR spectroscopy, we can deduce that gelation and secondary structural changes start immediately and some

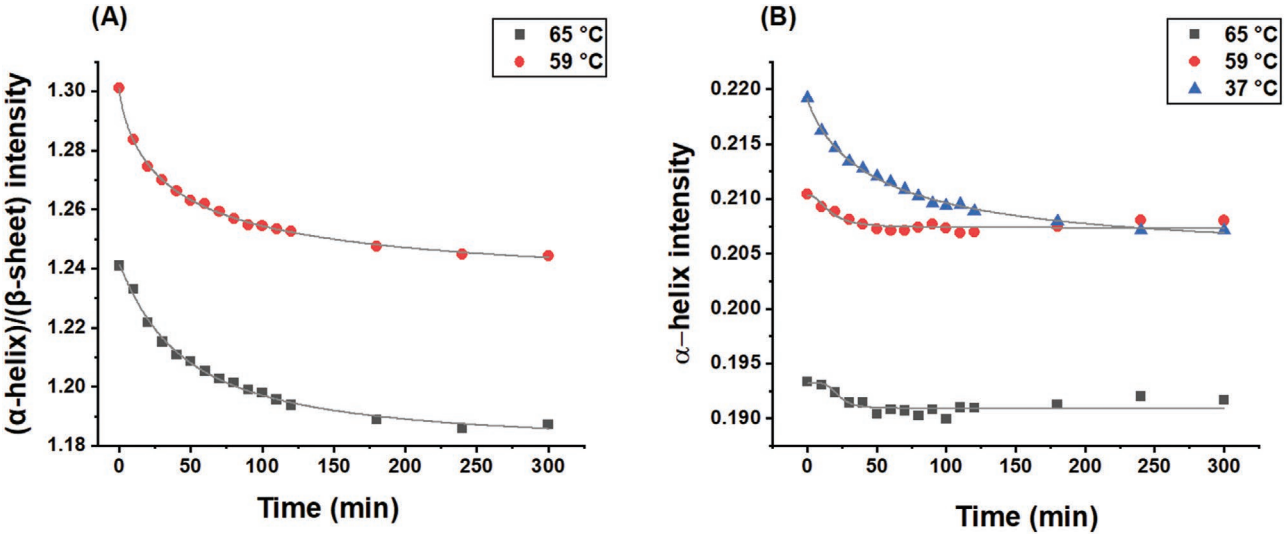

Figure 4. Time dependence of the A) I(α-helix)/I(β-sheet) for BSA precursor solution at 65 °C (black) and 59°C (red), pH 7 and B) α-helices intensity of 3×10^{-3} M BSA precursor solution at 65 °C (black), 59 °C (red) and 37 °C (blue, pH 3.5). All gray lines are fitted curves.

oligomers might be formed in this initial time period below 1 h. After initiation of gel formation, the secondary structure keeps changing in a slower way, which could be due to the robustness of the hydrogel and hindered diffusion. Further information about the potential effects of fatty acid on gelation is available in the Supporting Information.

3.4. 16-DSA Release Studies from BSA Hydrogels

It has been found using different techniques that BSA possesses 7 long-chain fatty acid binding sites with diverse affinities in its native form.[44,45] By performing EPR spectroscopic measurements it is possible to gain insights into the albumin–FA interaction, binding process, and degree of motional freedom within the binding pocket and of the protein.[24,29] Furthermore, the EPR (absorption) signal intensity can be determined by double integration of the first-derivative CW EPR spectrum.[46] Results from recent investigations on the bound states of spin labeled FA loaded into BSA and HSA hydrogels illustrate that not only the proteins individually but also their hydrogels have strong FA binding capacities, with differences in the number and strength of the binding depending on the preparation of the hydrogels.[14] Next, we discuss the effect of different gel preparation methods and incubation time on the release rate of 16-DSA as a drug model from BSA hydrogels. We elaborate on the EPR spectroscopic results obtained from release tests for different samples.

Different spectroscopic components of a multimodal 16-DSA EPR spectrum, namely freely tumbling 16-DSA, 16-DSA intermediately and strongly bound can be distinguished in the EPR spectra and are shown separately in **Figure 5**A, while Figure 5B displays various regions of the EPR spectrum for pure 16-DSA in buffer. Figure 5C,D are examples of EPR spectra obtained from release test for thermally induced hydrogels (other EPR spectra are available in Figure S5, Supporting Information).

Figure 6 displays the 16-DSA release profiles from BSA hydrogels with different 16-DSA:BSA molar ratios prepared by both preparation methods. The release curves for different samples in PBS buffer are analyzed by plotting the double integral of the EPR spectra against various time intervals (the release curves for hydrogels prepared with lower incubation times are available in Figure S6, Supporting Information). According to the shape of the curves in Figure 6, all three hydrogels with three different concentrations of the fatty acid show an initial burst release during the first 24 h, which is followed by a sustained release over long time periods later. The first and faster release phase is due to the diffusion of PBS medium into the protein matrix, which can dissolve the entrapped spin probe close to or at the surface of the hydrogels. However, the amount of model drug in the inner part of the protein matrix is depleted and the hydrogel possibly loses its integrity at some point of time which leads to the observed burst release. In addition, in Figure 6 we observe the effect of initial 16-DSA loading on the release profile from different hydrogels. We find that the increase in the model drug contents results in a faster and higher release rate in all experimental systems (due to long preparation time, the $BSA_T(59,7)$ with 2:1 16-DSA:BSA molar ratio is not discussed).

Figure 7A,B shows the direct effect of changing the incubation time on the release profile for $BSA_T(65,7,t)$ and $BSA_p(37,3.5,t)$ (for $BSA_T(59,7,t)$ and a comparison between the release profiles of hydrogels prepared by different methods see the Supporting Information). The results of Figure 7 are in agreement with the rheological characterization and ATR IR data, as increasing the incubation time leads to mechanically more robust hydrogels; increasing the gelation time from 5 min to 1 h for $BSA_T(65,7)$ and 30 min to 1 h for $BSA_p(37,3.5)$ leads to lower release rate due to the higher mechanical strength of the hydrogel networks. Consequently, it is possible to alter the release rate by changing the incubation time and preparation methods, which indicate a remarkably straightforward potential for tuning BSA hydrogels for drug delivery applications.

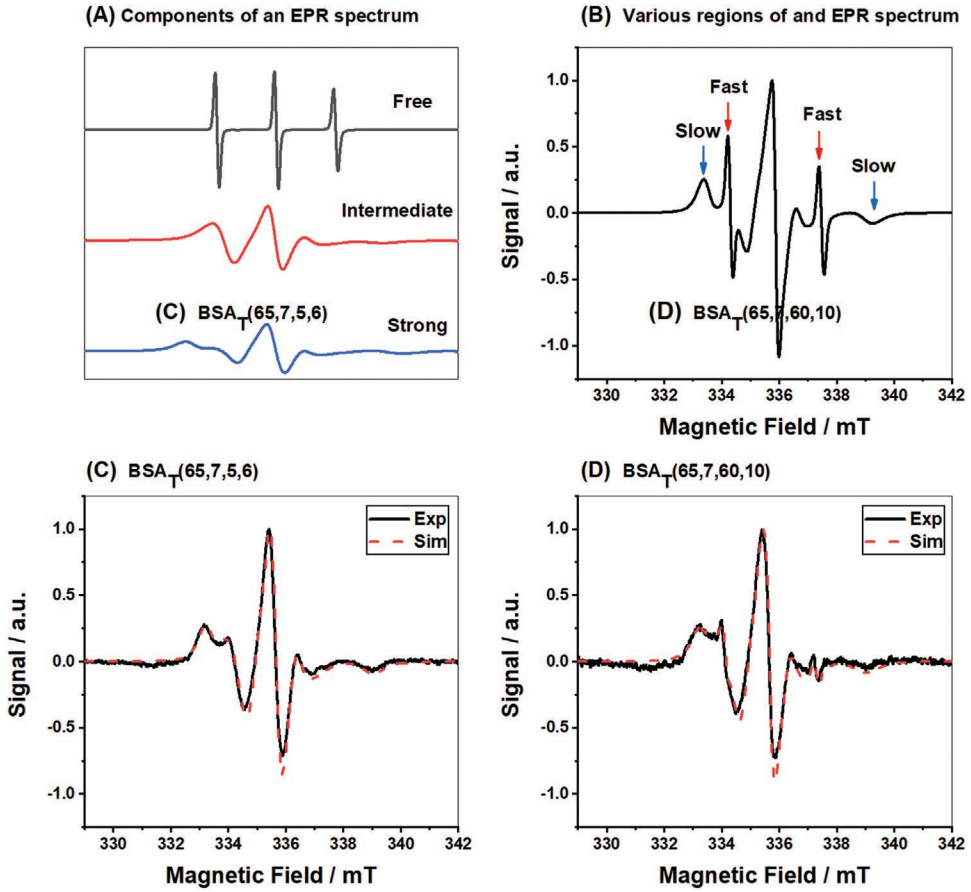

Figure 5. A) different components of an EPR spectrum, B) various regions of EPR spectrum for 16-DSA, C) BSA$_T$(65,7,5,6) at a 0.5:1 16-DSA:BSA molar ratio and D) BSA$_T$(65,7,60,10) at a 0.5:1 16-DSA:BSA molar ratio.

Figure 7 simply gives the number of released 16-DSA molecules, regardless of whether they float freely or are bound to albumin. **Figure 8** presents more molecular insights by showing the results obtained from spectral simulations, which give information on the relative percentages of tightly and intermediately bound 16-DSA to BSA and freely rotating 16-DSA. Figure 8A,B displays the interaction of FAs with BSA hydrogel during the release tests for the samples with a 0.5:1 16-DSA:BSA molar ratio with two different incubation times prepared by the thermally induced method at 65 °C. To compare the results quantitatively, we can use the simplified number of the rotational correlation time τ_c that can be calculated using diffusion tensor D obtained from EPR spectra simulation, $\tau_c = \frac{1}{6}(DxxDyyDzz)^{-\frac{1}{3}}$ which is in the range of 10 ps for fast tumbling molecules to a few microseconds (or lomger) for strongly immobilized, bound components.[47] In addition, information about the polarity around the nitroxide group can be determined from the isotropic ^{14}N-hyperfine coupling constant a_{iso}. Larger value of a_{iso} are indicative of highly polar environments (for 16-DSA in water, e.g., a_{iso} = 44.5 MHz) while lower polarity results in smaller hyperfine couplings (e.g., 16-DSA bound to BSA in solution has a_{iso} = 43.4 MHz).[48,49] These two parameters gained from the simulation of EPR spectra for different release systems are summarized in **Table 1**. As can be seen in Figure 8A,B almost 48% of 16-DSA is tightly bound to BSA in the released solution and 51% shows intermediate rotational motion at the beginning of the release test and there is no sign of freely rotating FAs being released from the hydrogel prepared by an incubation of only 5 min. However, by increasing the incubation time to 1 h the percentage of strongly bound 16-DSA decreases to 24% while that of the intermediately immobilized FAs to BSA increases to 72%. Moreover, for this sample almost 3% of 16-DSA rotates freely during the initial hours of release. This could be due to higher incubation times leading to more rigid networks (see the rheological characterization section), in which less albumin derivatives (individual albumin molecules and aggregates) can be released. Hence, more freely tumbling and intermediately bound FAs in buffer medium are found for these hydrogels while more strongly bound 16-DSA (in the binding pockets of BSA) can be released from hydrogels with lower incubation times because of looser gel structures that allow release of BSA, in which FAs are transported.

These EPR results provide a deeper insight at the molecular level and are in agreement with conclusions from rheological characterization and IR data. The effect of other 16-DSA:BSA molar ratios, incubation times and preparation methods on the release tests, the simulated CW-EPR spectra and the interaction of FA with BSA are described in more detail in the Supporting Information.

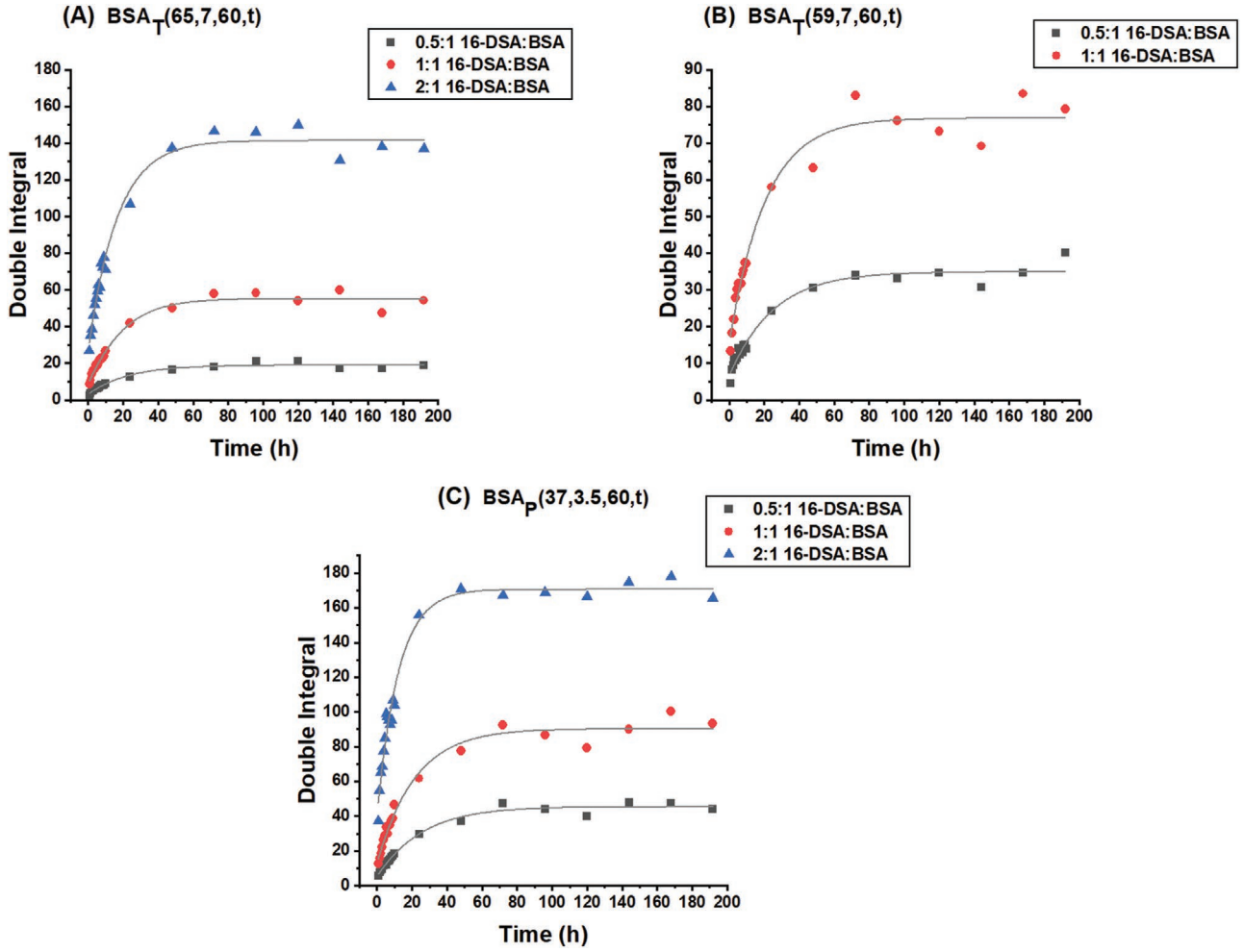

Figure 6. Double integral values versus release time intervals for A) BSA_T(65,7,60) hydrogel with 0.5:1, 1:1 and 2:1 16-DSA:BSA molar ratios, B) BSA_T(59,7,60) hydrogel with 0.5:1 and 1:1 16-DSA:BSA molar ratios and C) BSA_p(37,3.5,60) hydrogel with 0.5:1, 1:1 and 2:1 16-DSA:BSA molar ratios The gray lines are fitted curves and are meant as guide to the eye.

3.5. Dynamic Light Scattering Measurements

We use dynamic light scattering (DLS) to explore the size of the particles released over time based on the hydrodynamic radius and intensity time correlation function. **Figure 9** shows the autocorrelation functions obtained from DLS measurements during release from thermally induced hydrogels prepared at 65 °C and from pH triggered gels at 37 °C (the other 16-DSA:BSA molar ratios of these samples and BSA_T(59,7) are shown in the Supporting Information). Based on Figure 9, all autocorrelation functions display pronounced and significant y-intercept values, indicating the existence of well-defined particles in the release medium. Figure 9A shows that there is no significant difference in the decay curves of the autocorrelation functions for samples prepared with the same incubation time but different release times, implying the presence of at least one released component with the same size at any moment in time. However, we can clearly see the effect of the release time on the size of the released particles for hydrogels made with different incubation times (difference between 5 and 60 min incubation in Figure 9A). We find that samples with lower incubation times (5 min in case of the heat induced gel at 65 °C and 30 min for pH triggered hydrogel at 37 °C) display slower decays which correlates with the release of larger structures. Figure 9B shows the same behavior for lower incubation times, however the *y*-intercept value of the autocorrelation function decreases for higher incubation time and release after 192 h, which indicates a decrease in the scattering intensity. This could be due to the dissolution of the hydrogel by acidic condition and the existence of huge particles which leads to the delayed decay of autocorrelation function. These results are comparable with the rheological characterization and CW-EPR spectra, as hydrogels with lower incubation times are mechanically weak (see the rheology section), in which more albumin derivatives can be released. The simulation data of the EPR spectra suggest that the highest percentage of released particles from gels with lower incubation times stems from 16-DSA strongly attached to BSA. We can observe the same trend in the DLS measurements.

Besides the intensity time correlation function, we also observe the behavior of the hydrodynamic radius in order to compare different release tests in terms of the particle size. Further information about the effect of incubation time on

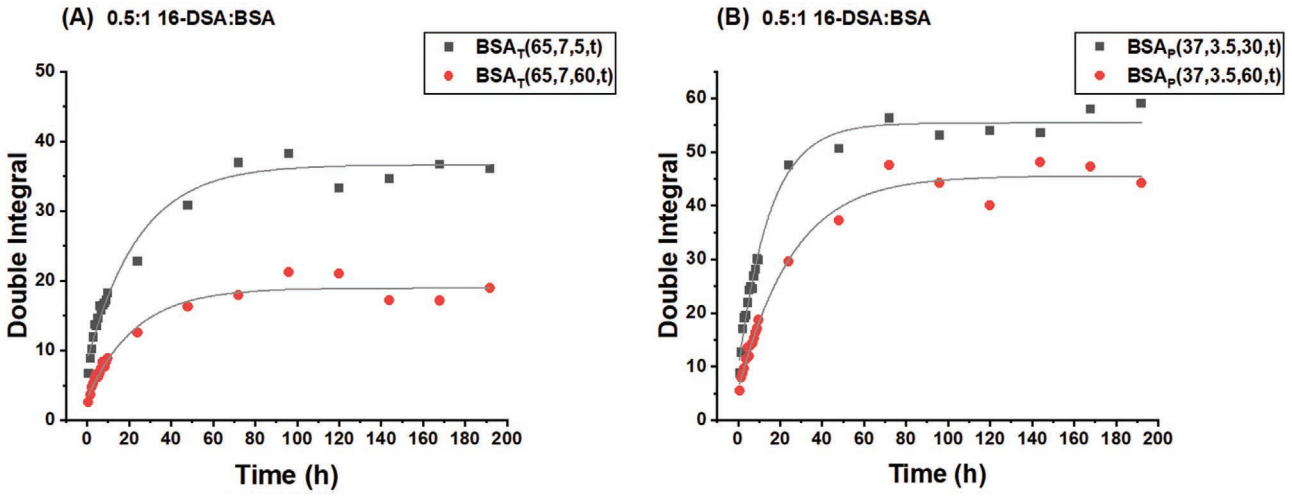

Figure 7. Double integral values versus release time intervals for 0.5:1 16-DSA:BSA molar ratio for A) thermally induced samples at 65 °C with two different incubation times of 5 and 60 min and B) pH-induced hydrogel at 37 °C with two different incubation times of 30 and 60 min. The gray lines are fitted curves and are meant as guide to the eye.

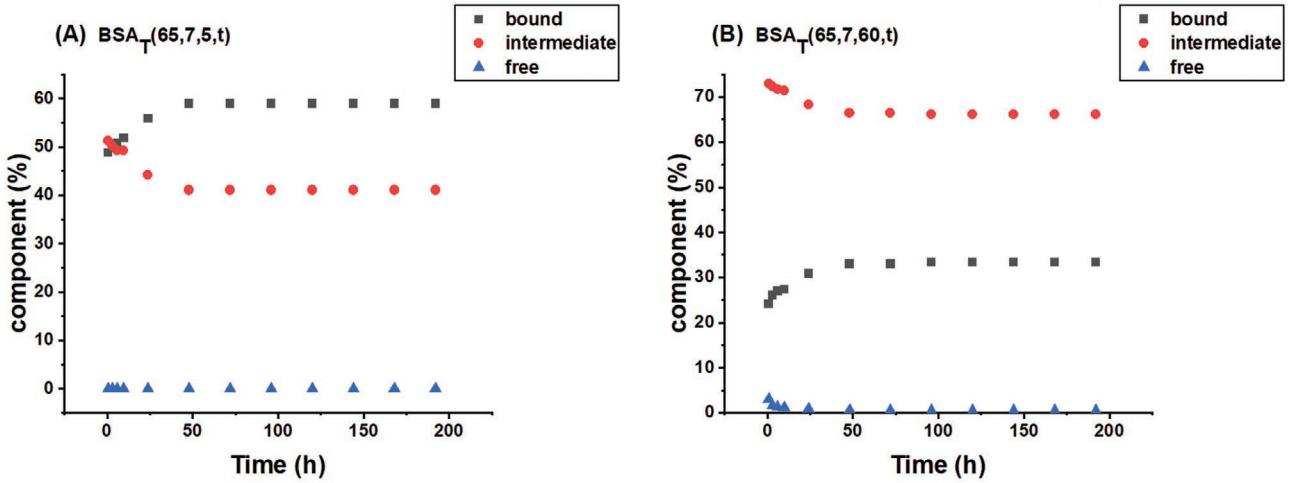

Figure 8. The released fractions of freely tumbling 16-DSA, strongly and intermediately bound 16-DSA to BSA against different time intervals for 0.5:1 16-DSA:BSA molar ratio of A) BSA$_T$(65,7,5) hydrogel and B) BSA$_T$(65,7,60) hydrogel.

the size of the released structures is given in the Supporting Information.

Figure 10 displays the autocorrelation functions of the release test after 3 h from thermally and pH induced hydrogels with (A) lower incubation times (5 and 30 min) and (B) higher incubation time (60 min) (other release time for these hydrogels are summarized in the Supporting Information). As can be seen in Figure 10A, all three autocorrelation functions show similar decays while increasing the incubation times to 60 min (Figure 10B) leads to more pronounced differences. It seems that intensity time correlation function of the hydrogel formed by pH induction decays later than of the gels prepared at 65 °C and 59 °C, which indicates the release of larger structures. As it was shown in rheology section, hydrogels prepared by lowering the pH to 3.5 displays the lowest mechanical strength compared to the ones synthesized by thermally induction methods. It is obvious that the pH-induced hydrogel has the highest release of strongly bound Fas, which are larger structures made from BSA in comparison with the release of 16-DSA alone or intermediately bound to BSA. On the other hand, the highest percentage of the components released from hydrogel prepared at 65 °C are attributed to the freely tumbling and intermediately BSA-bound FAs.

Table 1. Parameters obtained from simulation of Figure 8.

Figure	Release percentage of components during the first 45 min	Correlation time τc [ns]	Hyperfine coupling constant aiso [MHz]
A	48.7%	14	43.4
	51.2%	5.7	41.4
B	24.05%	15	43.4
	72.8%	5.7	42.3
	3.08%	0.11	44.5

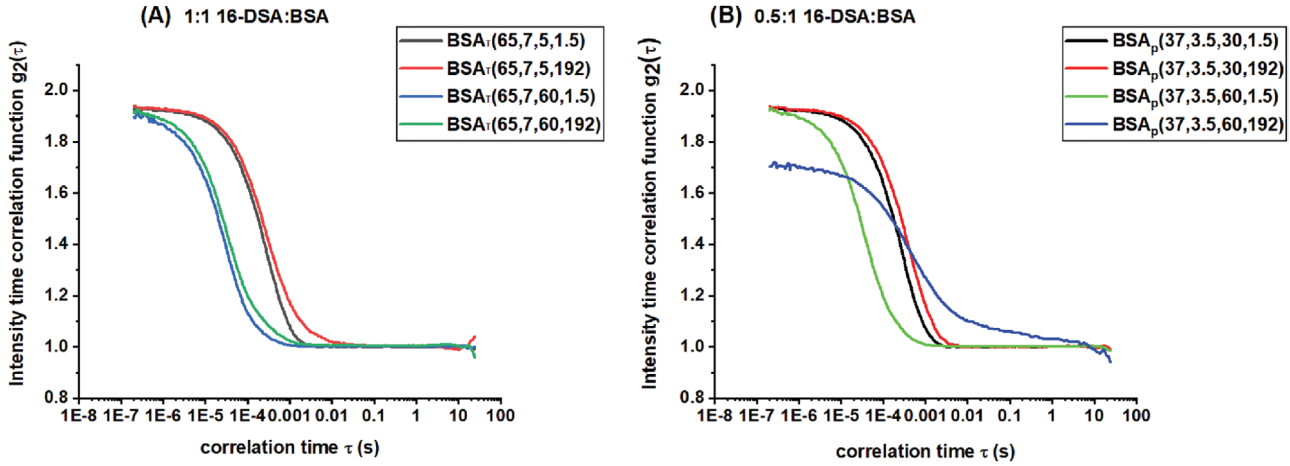

Figure 9. Intensity time autocorrelation functions of A) $BSA_T(65,7,5,t)$ and $BSA_T(65,7,60,t)$ at a 1:1 16-DSA:BSA molar ratio and B) $BSA_P(37,3.5,30,t)$ and $BSA_P(37,3.5,60,t)$ at a 0.5:1 16-DSA:BSA molar ratio.

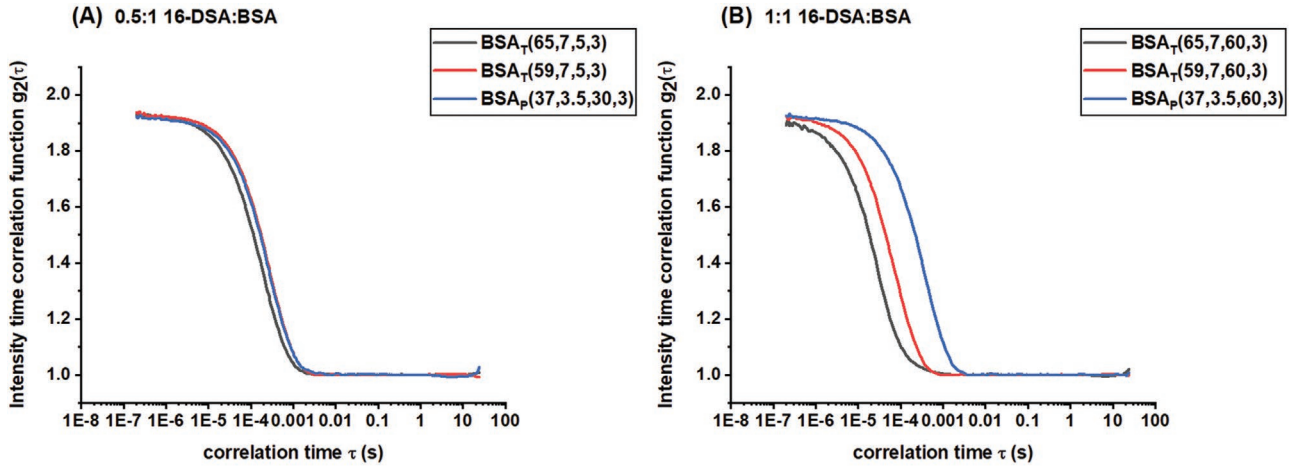

Figure 10. Intensity time autocorrelation functions for A) $BSA_T(65,7,5,3)$, $BSA_T(59,7,5,3)$ and $BSA_P(37,3.5,30,3)$ at a 0.5:1 16-DSA:BSA molar ratio and B) $BSA_T(65,7,60,3)$, $BSA_T(59,7,60,3)$ and $BSA_P(37,3.5,60,3)$ at a 1:1 16-DSA:BSA molar ratio.

4. Conclusions

In this study, we have prepared hydrogels from BSA to develop a controlled release system. The whole procedures of the gelation from bovine and human serum albumin via thermally and pH induced methods were described previously.[14] We have used the now established techniques for hydrogel preparation and the macroscopic properties such as viscoelastic behavior and the secondary structure changes during hydrogel formation were described in detail. Characterization of changes in the mechanical properties in the hydrogel (before complete dissolution) after the release tests remain on the agenda and will be part of a future study. The applicability of the synthesized hydrogels as delivery systems is analyzed by loading different molar ratios of the stearic acid derivative 16-DSA as a model drug into these structures. We have displayed that the release rate obtained from the double integral of EPR spectra depends principally on fatty acid concentration, incubation time, and gelation procedures. Higher 16-DSA ratios, lower incubation times and gel formation below the protein denaturation temperature lead to higher initial and sustained release rates. However, all the release patterns from different hydrogels independent of the mentioned parameters show initial burst release during the first 24 h followed by the sustained release over the later time periods.

Additionally, we are able to monitor the interaction of fatty acids with BSA hydrogels and characterize the size and nature of the released components using CW EPR spectroscopy and DLS measurements. The results suggest that a higher percentage of 16-DSA strongly bound to BSA is released from mechanically weak hydrogels due to expedited diffusion of water molecules into the gel network and subsequent release of unreacted (ungelated) albumins as dimers or individual proteins is significantly faster than from mechanically strong and nanoscopically tight hydrogel. We will in the future expand this approach to hydrogels triggered by partial denaturation through chemical addition (e.g. ethanol, see ref. [50]), which have yet different nanoscopic and mechanical properties.[50] We

hope that this research displays the potential of BSA hydrogels as suitable candidates for controlled drug delivery applications and will pave the way for their implementation in pharmaceutical applications.

Supporting Information

Supporting Information is available from the Wiley Online Library or from the author.

Acknowledgements

The authors thank Heike Schimm and Annekatrin Rother for technical support. This research was financially supported by the European Social Funds (ESF) and the State of Saxony-ANhalt through the graduate school AgriPoly.

Conflict of Interest

The authors declare no conflict of interest.

Keywords

albumin, electron paramagnetic resonance spectroscopy, fatty acid, hydrogel, release behavior

Received: April 13, 2020
Revised: May 11, 2020
Published online: June 22, 2020

[1] M. T. Larsen, M. Kuhlmann, M. L. Hvam, K. A. Howard, *Mol. Cell. Ther.* **2016**, *4*, 3.
[2] B. Elsadek, F. Kratz, *J. Controlled Release* **2012**, *157*, 4.
[3] Y.-J. Hu, Y. Liu, T.-Q. Sun, A.-M. Bai, J.-Q. Lü, Z.-B. Pi, *Int. J. Biol. Macromol.* **2006**, *39*, 280.
[4] K. Murayama, M. Tomida, *Biochemistry* **2004**, *43*, 11526.
[5] L. Zhang, Z. Lu, X. Li, Y. Deng, F. Zhang, C. Ma, N. He, *Polym. Chem.* **2012**, *3*, 1958.
[6] D. Zhao, X. Zhao, Y. Zu, J. Li, Y. Zhang, R. Jiang, Z. Zhang, *Int. J. Nanomed.* **2010**, *5*, 669.
[7] A. Sethi, M. Sher, M. R. Akram, S. Karim, S. Khiljee, A. Sajjad, S. N. Shah, G. Murtaza, *Acta Pol. Pharm.* **2013**, *70*, 597.
[8] N. Bhattarai, J. Gunn, M. Zhang, *Adv. Drug Delivery Rev.* **2010**, *62*, 83.
[9] J. Li, D. J. Mooney, *Nat. Rev. Mater.* **2016**, *1*, 16071.
[10] P. D. Reddy, D. Swarnalatha, *Int. J. PharmTech Res.* **2010**, *2*, 2025.
[11] E. Caló, V. V. Khutoryanskiy, *Eur. Polym. J.* **2015**, *65*, 252.
[12] N. A. Peppas, J. Z. Hilt, A. Khademhosseini, R. Langer, *Adv. Mater.* **2006**, *18*, 1345.
[13] L. Zhang, Z. Lu, X. Li, Y. Deng, F. Zhang, C. Ma, N. He, *Polym. Chem.* **2012**, *3*, 1958.
[14] S. H. Arabi, B. Aghelnejad, C. Schwieger, A. Meister, A. Kerth, D. Hinderberger, *Biomater. Sci.* **2018**, *6*, 478.
[15] K. Baler, R. Michael, I. Szleifer, G. A. Ameer, *Biomacromolecules* **2014**, *15*, 3625.
[16] J. I. Boye, I. Alli, A. A. Ismail, *J. Agric. Food Chem.* **1996**, *44*, 996.
[17] S. K. Baier, D. J. McClements, *J. Agric. Food Chem.* **2003**, *51*, 8107.
[18] Y. Sun, Y. Huang, *J. Mater. Chem. B* **2016**, *4*, 2768.
[19] K. Baler, O. A. Martin, M. A. Carignano, G. A. Ameer, J. A. Vila, I. Szleifer, *J. Phys. Chem. B* **2014**, *118*, 921.
[20] Z. Yu, M. Yu, Z. Zhang, G. Hong, Q. Xiong, *Nanoscale Res. Lett.* **2014**, *9*, 343.
[21] D. J. Lurie, K. Mäder, *Adv. Drug Delivery Rev.* **2005**, *57*, 1171.
[22] Y. Akdogan, M. Emrullahoglu, D. Tatlidil, M. Ucuncu, G. Cakan-Akdogan, *Phys. Chem. Chem. Phys.* **2016**, *18*, 22531.
[23] K. Mäder, G. Bacic, A. Domb, O. Elmalak, R. Langer, H. M. Swartz, *J. Pharm. Sci.* **1997**, *86*, 126.
[24] J. Reichenwallner, D. Hinderberger, *Biochim. Biophys. Acta, Gen. Subj.* **2013**, *1830*, 5382.
[25] Y. Aboul-Enein, A. Bunaciu, S. Fleschin, *Gazi Univ. J. Sci.* **2014**, *27*, 637.
[26] H. Yang, S. Yang, J. Kong, A. Dong, S. Yu, *Nat. Protoc.* **2015**, *10*, 382.
[27] M. Drescher, *EPR Spectroscopy: Applications in Chemistry and Biology*, Springer, Berlin **2012**.
[28] R. Graf, M. R. Hansen, D. Hinderberger, K. Muennemann, H. W. Spiess, *Phys. Chem. Chem. Phys.* **2014**, *16*, 9700.
[29] M. J. N. Junk, H. W. Spiess, D. Hinderberger, *Angew. Chem., Int. Ed.* **2010**, *49*, 8755.
[30] K. Widder, S. R. MacEwan, E. Garanger, V. Núñez, S. Lecommandoux, A. Chilkoti, D. Hinderberger, *Soft Matter* **2017**, *13*, 1816.
[31] J. Eisermann, L. Prager, D. Hinderberger, *Phys. Chem. Chem. Phys.* **2018**, *20*, 1421.
[32] J. Lim, S. P. Yeap, H. X. Che, S. C. Low, *Nanoscale Res. Lett.* **2013**, *8*, 381.
[33] M. Kaszuba, D. McKnight, M. T. Connah, F. K. McNeil-Watson, U. Nobbmann, *J. Nanopart. Res.* **2008**, *10*, 823.
[34] A. Bootz, V. Vogel, D. Schubert, J. Kreuter, *Eur. J. Pharm. Biopharm.* **2004**, *57*, 369.
[35] J. Holoubek, *J. Quant. Spectrosc. Radiat. Transfer* **2007**, *106*, 104.
[36] A. P. Minton, *Anal. Biochem.* **2016**, *501*, 4.
[37] C. Yan, D. J. Pochan, *Chem. Soc. Rev.* **2010**, *39*, 3528.
[38] N. S. Hettiarachchy, G. R. Ziegler, *Protein Functionality in Food Systems*, CRC Press, Boca Raton, FL **1994**.
[39] A. A. Spector, *J. Lipid Res.* **1975**, *16*, 165.
[40] S. Gumpen, P. O. Hegg, H. Martens, *Biochim. Biophys. Acta, Lipids Lipid Metab.* **1979**, *574*, 189.
[41] T. Peters Jr, *All About Albumin: Biochemistry, Genetics, and Medical Applications*, Academic Press, Boca Raton, FL **1995**.
[42] K. Takeda, A. Wada, K. Yamamoto, Y. Moriyama, K. Aoki, *J. Protein Chem.* **1989**, *8*, 653.
[43] G. Navarra, D. Giacomazza, M. Leone, F. Librizzi, V. Militello, P. L. San Biagio, *Eur. Biophys. J.* **2009**, *38*, 437.
[44] G. J. van der Vusse, *Drug Metab. Pharmacokinet.* **2009**, *24*, 300.
[45] M. Fasano, S. Curry, E. Terreno, M. Galliano, G. Fanali, P. Narciso, S. Notari, P. Ascenzi, *IUBMB Life* **2005**, *57*, 787.
[46] S. Kempe, H. Metz, K. Mäder, *Eur. J. Pharm. Biopharm.* **2010**, *74*, 55.
[47] S. Van Doorslaer, G. Jeschke, *Fluxional Organometallic and Coordination Compounds*, Vol. 6, Wiley, New York **2005**.
[48] M. J. N. Junk, U. Jonas, D. Hinderberger, *Small* **2008**, *4*, 1485.
[49] M. J. N. Junk, W. Li, A. D. Schlüter, G. Wegner, H. W. Spiess, A. Zhang, D. Hinderberger, *Macromol. Chem. Phys.* **2011**, *212*, 1229.
[50] S. H. Arabi, D. Haselberger, D. Hinderberger, *Molecules* **2020**, *25*, 1927